

“Sunshade World”: a fully coupled GCM evaluation of the climatic impacts of geoengineering

Daniel J. Lunt^(1,2,*), Andy Ridgwell⁽¹⁾, Paul J. Valdes⁽¹⁾, Anthony
Seale⁽¹⁾

(1) BRIDGE
School of Geographical Sciences
University of Bristol
University Road
Bristol BS8 1SS
UK

(2) British Antarctic Survey
Geological Sciences Division
High Cross
Madingley Road
Cambridge CB3 0ET
UK

(*) Corresponding author:
Email: d.j.lunt@bristol.ac.uk
Tel: +44 (0) 117 3317483
Fax: +44 (0) 117 9287878

Abstract

Sunshade geoengineering - the installation of reflective mirrors between the Earth and the Sun to reduce incoming solar radiation, has been proposed as a mitigative measure to counteract anthropogenic global warming. Although the popular conception is that geoengineering can re-establish a 'natural' pre-industrial climate, such a scheme would itself inevitably lead to climate change, due to the different temporal and spatial forcing of increased CO₂ compared to reduced solar radiation. We investigate the magnitude and nature of this climate change for the first time within a fully coupled General Circulation Model. We find significant cooling of the tropics, warming of high latitudes and related seaice reduction, a reduction in intensity of the hydrological cycle, reduced ENSO variability, and an increase in Atlantic overturning. However, the changes are small relative to those associated with an unmitigated rise in CO₂ emissions. Other problems such as ocean acidification remain unsolved by sunshade geoengineering.

1 Introduction

Geoengineering can be defined as the “intentional large-scale manipulation of the environment” (Keith, 2000) and has been considered for the mitigation of climate change in response to elevated anthropogenic greenhouse gas emissions (IPCC, 2007). Various schemes have been proposed, including the injection of sulphate aerosols into the atmosphere (Crutzen, 2006) and increasing carbon sinks through oceanic iron fertilisation (Martin, 1990). Early (1989) proposed the implementation of a space-based “sunshade”, situated at the Lagrange point (L1) between the Earth and the Sun, designed to reduce solar insolation. The feasibility of such a sunshade was assessed by Angel (2006), who concluded that it could be developed and deployed in about 25 years at a cost of a few trillion dollars, while others have assessed ethical considerations (e.g. Jamieson, 1996; Bodansky, 1996). Here we focus on the the climatic impacts of sunshade geoengineering.

The purpose of sunshade geoengineering is to reduce the incident solar radiation at the top of the atmosphere, in order to offset the surface warming caused by increased atmospheric greenhouse gas concentrations. However, although the global annual mean temperature could in theory be reduced to exactly that characterising pre-industrial climate, the differing spatial and temporal distributions of the solar and CO₂ forcings would result in residual differences in climate between the “Sunshade World’ and pre-industrial. In this study, we calculate the nature and magnitude of this residual climate change.

Analogous experiments have been carried out previously by Govindasamy and Caldeira (2000), Govindasamy et al (2003), henceforth G2003, and Matthews and Caldeira (2007). However, all these studies were carried out with models of reduced complexity. Govindasamy and Caldeira (2000) and G2003 used a full complexity atmospheric model, but in conjunction with a ‘slab’ ocean, which is not capable of predicting changes in ocean circulation and heat transport, and includes a relatively simple representation of seaice. Matthews et al (2007) used a fully coupled atmosphere-ocean model, but with a reduced complexity (energy-moisture balance, EMB) atmosphere. Although atmospheric

38 EMB models provide useful insights into spatial distributions of temperature change and timescales of
39 response of the system to perturbations, they are not capable of representing changes in atmospheric
40 circulation and moisture transport (Weaver et al, 2001). Both Govindasamy and Caldeira (2000) and
41 G2003 recommended that future work should be carried out using models which have a fully coupled
42 and dynamic representation of oceans and seaice, and associated feedbacks. This is the challenge
43 which we address here.

44 **2 Experimental Design**

45 We use the fully coupled atmosphere-ocean UK Met Office GCM, HadCM3L (Cox et al, 2000).
46 HadCM3L has a horizontal resolution on 3.75° longitude by 2.5° latitude in the atmosphere and ocean,
47 19 vertical levels in the atmosphere and 20 vertical levels in the ocean. It consists of a hydrostatic
48 primitive equation atmosphere, with parameterisations for subgridscale processes such as convection
49 (Gregory and Rowntree, 1990) and boundary layer turbulence (Smith, 1993). The ocean includes pa-
50 rameterisations of eddy mixing (Gent and McWilliams, 1990), and a dynamic-thermodynamic seaice
51 scheme (Cattle and Crossley, 1995). The configuration of the model is identical to that described by
52 Lunt et al (2007), except that we use a more recent version of the land-surface scheme (MOSES2.2),
53 with fixed prescribed modern vegetation.

54 We carried out three 220-year simulations, all initialised from the end of a spin-up totaling more
55 than 1000 years. The first is a pre-industrial control (*Pre*), the second has atmospheric CO_2 set at
56 1120 ppmv, $4\times$ the pre-industrial value (*Fut*), and the third has $4\times\text{CO}_2$ and a reduced solar constant
57 (*Geo*). In simulation *Geo*, we reduced the solar constant such that the global annual mean 2 m air
58 temperature was as close as possible to that of the *Pre* simulation. This was achieved by first carrying
59 out a preparatory simulation with a first estimate for the required reduction. This was refined twice
60 by assuming a linear relation between applied forcing and surface temperature change. As a result,

61 simulation *Geo* has a solar constant 57 Wm^{-2} smaller than that of *Pre*, a reduction of 4.2%. For
62 comparison, G2003 found that they required a reduction of 3.6% to offset a $4\times$ increase in CO_2 .

63 The timeseries of global annual mean 2 m air temperature (T_{2m}) in simulations *Pre*, *Geo* and *Fut* is
64 shown in Figure 1. In the following sections, the results of the last 60 years of these simulations are
65 described and discussed. Over this period, the average of T_{2m} is 12.78°C in simulation *Pre*, 12.77°C
66 in simulation *Geo*, and 17.24°C in simulation *Fut*. The close agreement in T_{2m} between the *Pre*
67 and *Geo* values (0.01°C) compares with a difference of 0.07°C obtained by G2003. We have thus
68 produced a climate that is indistinguishable from pre-industrial when viewed from the widely used
69 metric of global mean surface air temperature.

70 **3 Results**

71 The 1-dimensional energy balance structure of the Sunshade World is rather different to that of the pre-
72 industrial. At the top of the atmosphere, the applied decrease in incoming solar radiation (14.2 Wm^{-2})
73 is balanced by a reduction in outgoing solar radiation (6.8 Wm^{-2} , about 2.6 Wm^{-2} of which is due
74 to an decrease in planetary albedo), and a decrease in outgoing long wave radiation (7.5 Wm^{-2}). The
75 decrease in outgoing long wave radiation is due to a colder upper atmosphere in the geoengineered
76 world, due largely to the increased CO_2 and partly due to the reduction in incoming solar radiation. At
77 the surface, the decrease in downwards solar radiation (5.5 Wm^{-2}) is balanced largely by a decrease
78 in latent heat of evaporation (4.4 Wm^{-2}), and a decrease in upwards solar radiation (0.9 Wm^{-2} , about
79 0.2 Wm^{-2} of which is due to an decrease in surface albedo). The decrease in latent heat is related to
80 a cooler tropical ocean in the geoengineered climate (see below).

81 Although we have tuned the solar constant in simulation *Geo* so that the value of T_{2m} is near identical
82 to that of *Pre*, climate differs markedly regionally between the two simulations. For example, there
83 is a warming in surface air temperature at high latitudes in *Geo* compared to *Pre*, and a cooling in

84 the tropics (Figure 2a). This is due to the fact that a percentage reduction in solar insolation leads to a
85 latitudinal distribution of absolute solar forcing due to the curvature of the Earth, with greater forcing
86 towards the equator, and less towards the poles. The 4.2% reduction applied leads to an annual mean
87 TOA forcing of -17 Wm^{-2} at the equator and -7 Wm^{-2} at both poles. However, the forcing due to
88 the increased atmospheric CO_2 in simulation *Geo* does not have the same latitudinal structure. It is
89 greatest at the equator and less at high latitudes (following the patterns of surface temperature), but
90 the latitudinal gradient is less steep than for the solar forcing, and not symmetric across the equator,
91 with a minimum over Antarctica (Forster et al, 2000). Combining the solar and CO_2 forcing gives
92 a negative forcing at the equator, and a positive forcing at the poles. This is reflected in the surface
93 air temperature response. Spatially, 74% of the annual mean temperature changes are statistically
94 significant at a 5% confidence limit, as given by a Student t-test (Figure 2a), in comparison with
95 24% in G2003. Some of this difference is likely due the greater length of averaging period in our
96 simulation (60 years, compared with 15 years in G2003).

97 The temperature response is not directly proportional to the applied forcing, due to non-linear ampli-
98 fication of the forcing by positive feedbacks in the system, and a redistribution of heat due to changes
99 in atmospheric and ocean circulation. The maximum increase in surface temperature is in the Beau-
100 fort and East Siberian Seas, north of Alaska and Siberia, which is associated with a decrease in seaice
101 coverage (Figure 2b). The maximum decrease in surface air temperature occurs in the south east
102 Atlantic, off the west coast of Angola and Namibia. Here, the amplified signal is due to an increase
103 in upwelling, and shoaling of the thermocline in the tropics.

104 Another interesting impact of the sunshade is a slight decrease in temperature in the Barents Sea.
105 In the *Pre* simulation, this region is kept relatively warm due the presence of the Gulf Stream. In
106 simulation *Geo*, there is a reduction in the the intensity of the Gulf Stream, which results in a cooling
107 in the Barents Sea, associated with a slight increase in seaice. As expected, the poleward heat transport
108 in both hemispheres is reduced; changes to the atmospheric heat transports (maximum of 0.18 PW)
109 dominate over changes to the ocean heat transport (maximum of 0.09 PW).

110 As well as spatial differences, there are temporal differences between the temperature in Sunshade
111 World and pre-industrial. There is a reduction in the amplitude of the seasonal cycle; the seasonal
112 temperature range (Northern Hemisphere, JJA minus DJF) decreases by 0.3°C in the tropics, 0.4°C
113 in the subtropics and mid latitudes, and 1.5°C in the high latitudes relative to pre-industrial. This is
114 because the applied solar forcing has a strong seasonal component due to the curvature of the earth
115 (see G2003, Figure 1, bottom panel), which acts in a direction so as to reduce seasonality, whereas
116 the balancing due to the increase in CO₂ is more stable throughout the year, due largely to the heat
117 capacity of the oceans. We do not simulate a large change in the amplitude of the diurnal cycle in
118 simulation *Geo* relative to *Pre*, in agreement with G2003.

119 We also find important differences in the hydrological cycle, with Sunshade World generally drier
120 than the pre-industrial (Figure 2c). The global annual mean precipitation decreases by 5%; the largest
121 absolute decreases are in the tropics, and are related to the cooler and therefore less evaporative
122 tropical surface ocean. In addition, there is a northwards shift of the Inter-Tropical Convergence Zone
123 (ITCZ), which leads to increased precipitation just north of the equator in the Atlantic and eastern
124 Pacific. Despite the reduction in meridional temperature gradient, and an associated decrease in the
125 intensity of the northern Pacific storm track, the large scale precipitation changes in mid and high
126 latitudes are small. Perhaps counter-intuitively, the decreased precipitation in the tropics does not
127 lead to a decrease in soil moisture. Because evaporation also decreases due to the lowered surface
128 temperature, there is in fact a small increase in soil moisture. So the decreased precipitation may not
129 be likely to have a detrimental effect on food production in the tropics.

130 The dynamic ocean component of HadCM3L allows us to assess possible impacts on ENSO of the
131 geoengineered climate due to the reduction of insolation in the tropics. Figure 3 shows a timeseries of
132 surface air temperature in El Niño region 3.4, in the preindustrial and Sunshade World. The expected
133 reduction in annual mean temperature is apparent in the geoengineered timeseries, but there is also
134 a decrease in the variability. The standard deviation is 0.46°C in simulation *Pre* and 0.35°C in
135 simulation *Geo*. Fourier analysis of the two timeseries does not indicate a shift in the dominant ENSO

136 timescale. The decrease in the intensity of the ENSO signal is most likely due to the cooler tropical
137 SSTs and associated reduced tropical convection. This reduces the strength of the positive feedback
138 which in *Pre* acts to intensify El Niño events by increasing the strength of Walker circulation and
139 further amplifying the tropical SST anomaly.

140 We have also assessed the response of the thermohaline circulation to the sunshade geoengineering.
141 In many of the future climate GCM simulations of the IPCC, there is a reduction in the strength of
142 the Atlantic MOC (Meridional Overturning Circulation) relative to pre-industrial (IPCC, 2007). This
143 feature is also predicted in our *Fut* simulation, with a maximum reduction of 5 Sv. The main cause of
144 this is an increase in northwards moisture transport in the warmer climate, which reduces the density
145 of the surface waters in the North Atlantic, resulting in decreased overturning. In contrast, we find
146 that the circulation in simulation *Geo* is characterised by a slight increase in overturning (maximum
147 1.6 Sv) compared to pre-industrial, due to a reduction in northwards moisture transport due to the
148 cooler tropics. The impact of the sunshade thus has the opposite effect to the CO₂ forcing, and tends
149 to stabilise rather than destabilise the Atlantic MOC.

150 **4 Discussion**

151 Although HadCM3L has been used in many studies of future and paleo climates (e.g. Cox et al, 2000;
152 Lunt et al, 2007), it has reduced resolution compared to the most recent version (HadGEM) of the
153 UK Met Office used in the recent IPCC assessment report (IPCC, 2007), which may affect some of
154 our results. For instance, we have not found a large change in the characteristics of the storm tracks,
155 despite a weakening of the meridional temperature gradient in the model. It may be that a higher
156 resolution atmosphere model would predict a different response of the storm track, and hence large
157 scale winter precipitation in the Northern Hemisphere. We use HadCM3L here because of its relative
158 computational efficiency, and more extensive tuning to modern climatology.

159 We have kept vegetation fixed at pre-industrial values throughout all the simulations, thereby neglect-
160 ing vegetation-climate feedbacks. It is possible that the high CO₂ in a geoengineered world would
161 lead to increased global NPP by CO₂ fertilisation (Govindasamy et al, 2002), and lead to shifts in
162 vegetation type due to CO₂ controls on competition between plants with C₄ and C₃ photosynthetic
163 pathways (Ehleringer et al., 1997). However, future vegetation changes are likely to be dominated by
164 anthropogenic land-use change - a factor we cannot predict with any confidence. We have therefore
165 chosen to keep all vegetation characteristics fixed.

166 One possible extension to this study would be to force the fully coupled model with a scenario of
167 anthropogenic greenhouse gas and aerosol emissions, in a similar way to Matthews et al (2007).
168 However, here too uncertainty in the future CO₂ emissions trajectory would have to be considered.
169 Matthews et al (2007) also investigated the likely consequences of a catastrophic failure of a geoengi-
170 neering scheme, and found that in such a scenario, the climate would warm 20 times quicker than the
171 current anthropogenic warming - it is important that the consequences of such a rapid warming be
172 investigated with a fully dynamic model.

173 **5 Conclusions**

174 To our knowledge, this is the first analysis of sunshade geoengineering using a complex GCM with
175 a fully coupled atmosphere and dynamic ocean, an analysis that could also be applied to injection of
176 sulphate aerosols into the upper atmosphere. Compared to the pre-industrial, we find that a sunshade
177 geoengineered world with an identical global annual mean surface temperature has a reduced merid-
178 ional temperature gradient, and cooler tropics. There is a reduction in the intensity of the hydrological
179 cycle, in particular in tropical regions. This is all in agreement with previous work from a slab ocean
180 model (G2003). However, one of the main differences between this work and previous studies is that
181 we simulate a significant decrease in Arctic seaice in the sunshade geoengineered world. We also

182 predict a decrease in the seasonality relative to pre-industrial. Furthermore, the use of a fully dynamic
183 ocean in this study allows analysis of the ENSO and thermohaline circulation of the geoengineered
184 climate - we find a reduction in the amplitude of ENSO, and a slight increase in the strength of the
185 Atlantic MOC, relative to pre-industrial.

186 Despite significant differences in temperature and seaice in *Geo* relative to the pre-industrial, com-
187 pared to *Fut* (2d,e) the predicted changes are relatively small. *Fut* is globally 4.5°C warmer than
188 *Pre*, and 8.8°C warmer at high latitudes; for comparison, *Geo* is 0.8°C warmer at high latitudes.
189 Similarly, although we find significant decreases in precipitation in *Geo*, they are small compared to
190 the precipitation changes associated with the warmer climate of *Fut* (Figure 2f). In this respect, we
191 find that the sunshade geoengineering is highly successful. However, other direct effects of increased
192 CO₂ remain unmitigated, in particular ocean acidification and the subsequent impact on ecosystems.
193 Because of this, we can not recommend sunshade geoengineering as an alternative to the reduction
194 of emissions. This is even before the high cost, and possible ethical considerations, of a sunshade
195 geoengineering scheme have been considered.

196 Finally, it is interesting to note that the combination of reduced solar forcing and high CO₂ has been
197 present before, in the geological past. The reduction in solar constant of 4.2% (57 Wm⁻²) is similar
198 to that of the Middle Cambrian (Clough et al, 1981); at this time, it is also likely that CO₂ levels
199 were higher than pre-industrial (Royer, 2006). Therefore, geoengineering a future climate - Sunshade
200 World - characterised by reduced solar forcing and elevated CO₂, in terms of the gross radiation balance
201 could be likened to turning the clock back to the Cambrian World.

202 **6 Acknowledgments**

203 This work was carried out in the framework of the British Antarctic Survey GEACEP (Greenhouse to
204 ice-house: Evolution of the Antarctic Cryosphere And Palaeoenvironment) programme. DJL is also
205 part-funded by an RCUK (Research Councils UK) Fellowship. AJR is funded by the Royal Society.

206 **7 References**

- 207 Angel, R. (2006), Feasibility of cooling the Earth with a cloud of small spacecraft near the inner
208 Lagrange point (L1), Proceedings of the National Academy of Sciences, 103, 17184-17189.
- 209 Bodansky, D. (1996). May we engineer the climate?, Climatic Change, 33, 309-321.
- 210 Cattle, H. and Crossley, J. (1995), Modelling Arctic climate change, Philos Trans R Soc Lond A, 352,
211 201-213.
- 212 Clough, D.O. (1981). Solar interior structure and luminosity variations, Solar Physics, 74, 21-34.
- 213 Cox, P.M., Betts, R.A. Jones, C.D., Spall, S.A. and Totterdell, I.J. (2000), Acceleration of global
214 warming due to carbon-cycle feedbacks in a coupled climate model, Nature, 408, 184-187.
- 215 Crutzen, P. (2006), Albedo enhancement by stratospheric sulphur injections: a contribution to resolve
216 a policy dilemma? Climatic Change, 77, 211-219.
- 217 Early, J.T. (1989), Space-based Solar Screen to Offset the Greenhouse Effect, Journal of the British
218 Interplanetary Society, 42, 567-569.
- 219 Ehleringer, J.R., Cerling, T.E., Helliker, B.R. (1997), C4 photosynthesis, atmospheric CO2 and cli-
220 mate, Oecologia, 112, 285-299.
- 221 Forster, P.M., Blackburn, M., Glover, R., Shine, K.P. (2000), An examination of climate sensitiv-
222 ity for idealised climate change experiments in an intermediate general circulation model, Climate
223 Dynamics, 16, 833-849.
- 224 Gent, P.R. and McWilliams, J.C. (1990), Isopycnal mixing in ocean circulation models, Journal of
225 Physical Oceanography, 20, 150-155.

- 226 Govindasamy, B. and Caldeira, K. (2000), Geoengineering Earth's radiation balance to mitigate CO2-
227 induced climate change, *Geophysical Research Letters*, 27, 2141-2144.
- 228 Govindasamy, B., Thompson, S., Duffy, P.B., Caldeira, K. and Delire, C. (2002), Impact of geoengi-
229 neering schemes on the terrestrial biosphere, *Geophysical Research Letters* 29, 2061, doi:10.1029/2002GL015911.
- 230 Govindasamy B, Caldeira, K. and Duffy, P.B. (2003), Geoengineering Earth's radiation balance to
231 mitigate climate change from a quadrupling of CO2, *Global and Planetary Change*, 37, 157-168.
- 232 Gregory, D. and Rowntree, P.R. (1990), A mass flux convection scheme with representation of cloud
233 ensemble characteristics and stability-dependent closure, *Monthly Weather Review*, 118, 1483-1506.
- 234 IPCC (2007). Solomon, S., Qin, D., Manning, M., Chen, Z., Marquis, M., Averyt, K.B., Climate
235 Change 2007: The Physical Science Basis. Contribution of Working Group I to the Fourth Assess-
236 ment Report of the Intergovernmental Panel on Climate Change, Cambridge University Press.
- 237 Jamieson, D. (1996), Ethics and intentional climate change, *Climatic Change*, 33, 323-336.
- 238 Keith, D.W. (2000), Geoengineering the climate: history and prospect, *Annual Reviews of Energy
239 and the Environment*, 25, 245-284.
- 240 Lunt, D.J., Ross, I., Hopley, P.J., Valdes, P.J. (2007), Modelling Late Oligocene C4 grasses and
241 climate, *Palaeogeography, Palaeoclimatology, Palaeoecology*, 251, 239-253.
- 242 Martin, J.H. (1990). Glacial-Interglacial CO2 change: The iron hypothesis, *Paleoceanography*, 5,
243 1-13.
- 244 Matthews, H.D. and Caldeira, K. (2007), Transient climate-carbon simulations of planetary geoengi-
245 neering, *Proceedings of the National Academy of Sciences*, 104, 9949-9954.

246 Royer, D.L. (2006), CO₂-forced climate thresholds during the Phanerozoic, *Geochimica et Cos-*
247 *mochimica Acta*, 70, 5665-5675.

248 Smith, R.N.B. (1993), Experience and developments with the layer cloud and boundary layer mix-
249 ing schemes in the UK Meteorological Office Unified Model, Proc. ECMWF/GCSS workshop on
250 parameterisation of the cloud-topped boundary layer, Reading, England.

251 Weaver, A.J., M. Eby, E. C. Wiebe, C. M. Bitz, P. B. Duffy, T. L. Ewen, A. F. Fanning, M. M. Holland,
252 A. MacFadyen, H.D. Matthews, K.J. Meissner, O. Saenko, A. Schmittner, H. Wang and M. Yoshimori
253 (2001), The UVic Earth System Climate Model: Model description, climatology and application to
254 past, present and future climates. *Atmosphere-Ocean*, 39, 361-428.

255 **8 Figure Captions**

256 Figure 1: Timeseries of global annual mean 2 m air temperature in simulations *Pre* (*black*), *Fut*
257 (*blue*), and *Geo* (*red*).

258 Figure 2: (a,b,c) Change in climatic parameters in Sunshade World relative to pre-industrial. (a) 2 m
259 air temperature ($^{\circ}\text{C}$), (b) seaice depth (m), and (c) precipitation (mmday^{-1}). (d,e,f) Change in climatic
260 parameters in the $4\times\text{CO}_2$ world relative to pre-industrial. (d) 2 m air temperature ($^{\circ}\text{C}$), (e) seaice
261 fraction (m), and (f) precipitation (mmday^{-1}). Dotted line shows those regions where the difference
262 is statistically significant at a 5% confidence limit, as given by a Student T test.

263 Figure 3: Timeseries of annual mean 2 m air temperature in El Niño region 3.4 in simulations *Pre*
264 (*black*) and *Geo* (*red*).

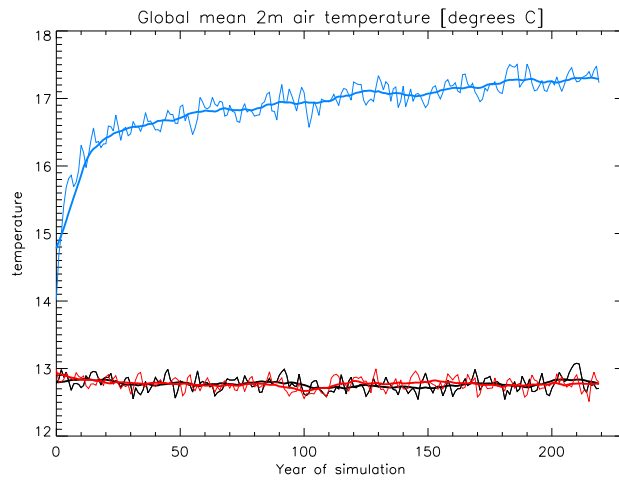


Figure 1: Timeseries of global annual mean 2 m air temperature in simulations *Pre* (black), *Fut* (blue), and *Geo* (red).

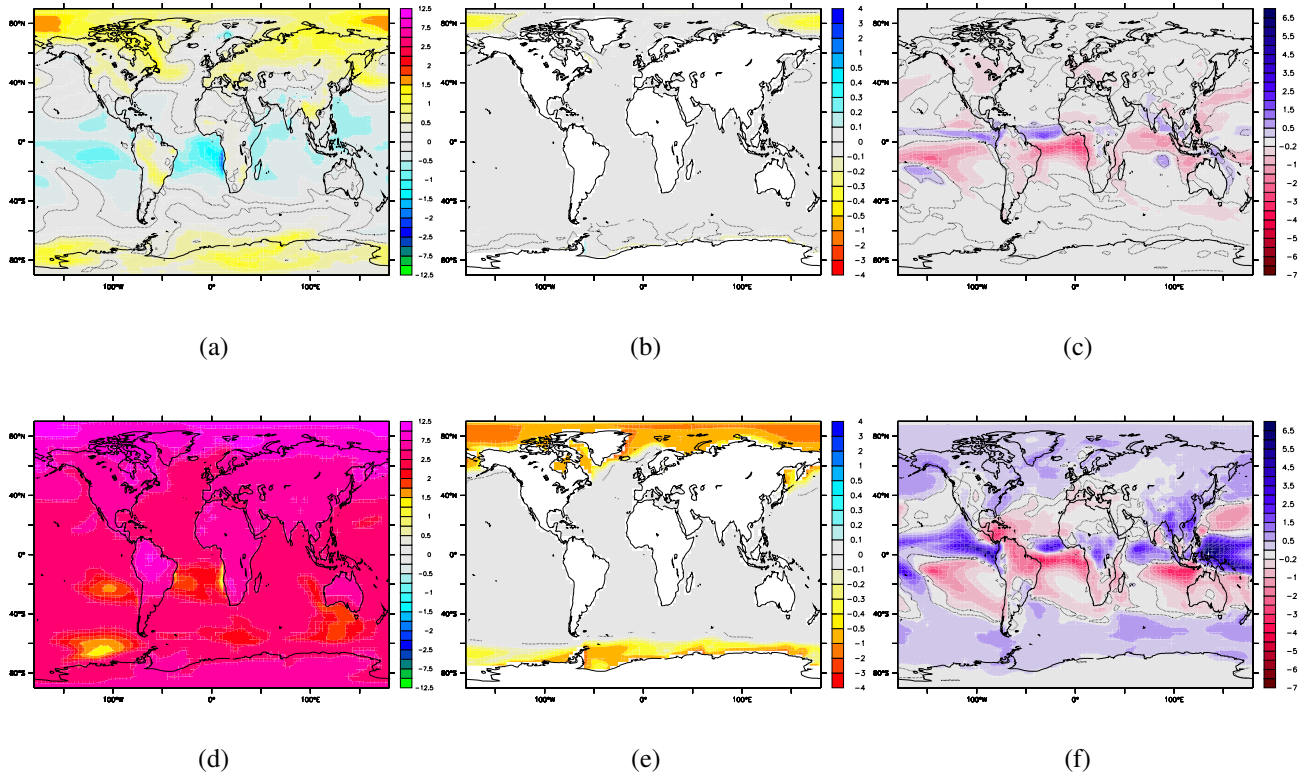


Figure 2: (a,b,c) Change in climatic parameters in Sunshade World relative to pre-industrial. (a) 2 m air temperature ($^{\circ}\text{C}$), (b) seaice depth (m), and (c) precipitation (mmday^{-1}). (d,e,f) Change in climatic parameters in the $4\times\text{CO}_2$ world relative to pre-industrial. (d) 2 m air temperature ($^{\circ}\text{C}$), (e) seaice fraction (m), and (f) precipitation (mmday^{-1}). Dotted line shows those regions where the difference is statistically significant at a 5% confidence limit, as given by a Student T test.

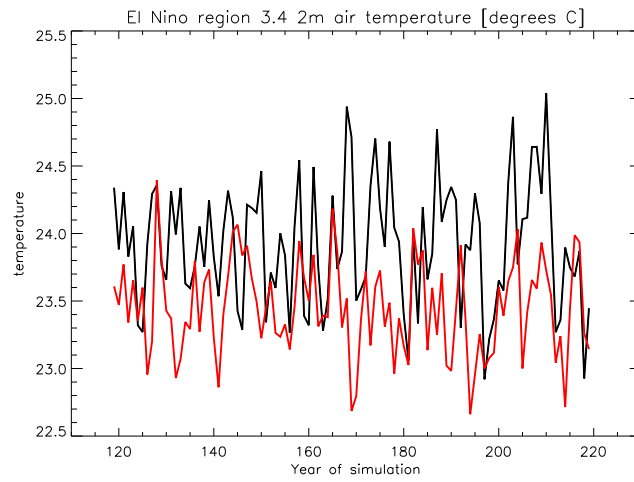


Figure 3: Timeseries of annual mean 2 m air temperature in El Niño region 3.4 in simulations *Pre* (black) and *Geo* (red).